Design of CFRP pre-stressed double-tee girders and experimental behavior under service load

Saverio Spadea[1], Marco Rossini[2], and Antonio Nanni[2]

[1] University of Dundee, Dundee, United Kingdom
[2] University of Miami, Coral Gables, USA

ABSTRACT: This paper deals with the design philosophy and the flexural performance under service loads of the precast pre-stressed girders constituting the deck of the Innovation Bridge, recently built at the University of Miami Campus. The two girders, cast in the shape of double-tees with shortened flange overhangs, were pre-stressed with seven-wire carbon FRP (CFRP) tendons and reinforced with basalt FRP (BFRP). CFRP strand have already been used for other pre-stressed or post-tensioned applications, but never before in large diameters for the fabrication of structural elements with thin cross-sections. Besides this, the selected percentage of the guaranteed capacity of the carbon FRP tendons applied at jacking was, for the first time, higher than the limit currently imposed by ACI 440.4R-04 guidelines. A load test was performed at the precast yard with concentrated loads corresponding to service condition, with the tested girder remaining un-cracked. The strains measured in the reinforcement and the detected deflections of the girder showed good agreement with the analytical predictions. Results show that CFRP pre-stressing technology can be successfully employed in thin walled concrete sections, over the thresholds suggested by current literature and without significant technological drawbacks.

1 INTRODUCTION

The Innovation Bridge consists of the following concrete elements: two precast pre-stressed girders, two cast-in-place pile caps, eight auger-cast piles, side blocks, back walls, deck topping, and curbs. Reinforcing bars comprise basalt FRP (BFRP) with an epoxy resin matrix and glass FRP (GFRP) with a vinyl ester matrix resin. Pre-stressing tendons are carbon FRP (CFRP) with an epoxy resin. Stainless steel is used for the bearing plates of the girders, the anchor bolts for the lampposts, and the railings. Novel fabrication technologies, including continuous closed stirrups and preassembled pile cages (Spadea et al. 2017) are also employed. As a result, there is not a single pound of carbon steel in any element of the bridge (Nanni et al. 2016).

The two girders are in the shape of double-tees (DTs) with shortened flange overhangs. The DTs are reinforced with BFRP and each stem is pre-stressed with nine CFRP strands. These kind of precast elements, commonly used as floors for parking garage structures, are particularly thin and efficient. Their employment in a pedestrian bridge allows to greatly simplify the construction process. It is not necessary to perform the in-situ casting of a separate deck, but only to overlay the precast elements with a concrete topping.

The pre-stressing of CFRP tendons remains a challenge because of the high sensitivity of the material to sharp machinery and shocks, which requires splicing with conventional steel strands, in order to allow the employment of currently available stressing systems. Previous examples of double-T girders included a lower number of CFRP tendons per stem. Either smaller diameters or thicker concrete sections were employed (Grace 2000; Ushijima et al. 2016).

2 MATERIALS

2.1 CFRP Tendons

Carbon Fiber Composite (CFCC) tendons comprising seven individual wires and manufactured by Tokyo Rope Manufacturing Co. Ltd., Japan, were employed. Each wire consists of carbon fibers impregnated with thermosetting epoxy resin and protected with wrapping material (polyester fiber). The strand has a 15.2 mm nominal diameter and a guaranteed strength (f_{pu}) of 2337 MPa. The nominal failure capacity guaranteed by the manufacturer is 270 kN, a value slightly higher than the conventional yield load of steel strands having the same nominal diameter. The CFCC high guaranteed tensile load allows high pre-stressing rate whereas the lower elastic modulus (148.9 GPa vs. 197.9 GPa the one exhibited by steel strands) causes reduced losses resulting from the elastic shortening and creep of concrete. The long-term relaxation losses are comparable to those exhibited by steel (Tokyo Rope Mfg Co Ltd 2014).

2.2 BFRP

Non-prestressed reinforcement used for the construction of the DTs comprises basalt fibers with an epoxy resin matrix (BFRP), manufactured by No Rust Rebar, Inc. (USA). The fibers are produced from basalt rock through a melting process. Due to their recent commercial availability, their use is not currently addressed by ACI 440 Committee. The characterization tests were performed at the University of Miami according to ACI 440.3R (2012) guidelines, following the methods currently used for other FRP reinforcements.

2.3 Concrete

A self-consolidating concrete (SCC) with specified compressive strength of 55 MPa, supplied by Titan America, was employed. The measured air content and spread of the fresh mix were respectively 1.0% and 635 mm. The average compressive strengths were measured at different times and used to compute the tensile strength of the concrete and its modulus of elasticity at different stages. The ACI 318 (2014) correlation formulae, together with the Florida DOT aggregate characterization factor, were employed.

3 DESIGN

The Innovation Bridge is designed with consideration to existing guides and technical reports dealing with the use of FRP reinforcement in concrete (AASHTO LRFD 2009; ACI 440.1R 2015; ACI 440.4R 2011). The two juxtaposed girders, nominally identical, are simply supported on a 20.11 m clear span, resulting in a total width of 4.34 m.

The design of CFRP PC elements is generally based on the assumptions traditionally adopted for steel PC. The most peculiar aspects to be considered are the brittle nature of the CFRP strands, their long-term behavior under imposed deformations, and their bond-to-concrete properties (Burke and Dolan 2001). Whereas steel tendons are typically stressed up to 85% of their yield stress (f_{sy}), allowable stresses in FRP tendons are limited to a sensibly lower percentage of their guaranteed ultimate strength (f_{pu}) to prevent possible rupture. According to ACI 440.4R, the recommended maximum jacking stress and maximum stress after the release of CFRP tendons should not exceed 65% and 60% of their ultimate strength, respectively.

The bridge is designed to remain un-cracked under a distributed live load of 4.8 kN/m^2 over its 75 years of service life. This load including dead weights results in a service maximum moment of 1284 kN·m and a maximum shear of 255.5 kN for each of the girders. This corresponds to an ultimate bending capacity demand of 1716 kN·m.

3.1 Details

The cross-section of the DT1 completed with concrete topping and curbs is shown in Figure 1. Furthermore, Figure 2 shows the top view of the precast element. The total depth of the precast section is 792 mm, with a flange thickness of 102 mm. Each stem of the DTs includes nine seven-wire CFRP tendons, tensioned with an initial pre-stressing force of 183.5 kN per strand before losses , hence, a total jacking force of 3303 kN with a 272 mm eccentricity was applied to each of the DTs. The deck was completed on-site with a 76 mm topping and, on the two sides, with a 356 mm × 356 mm curb, both cast with a 28 MPa specified strength concrete.

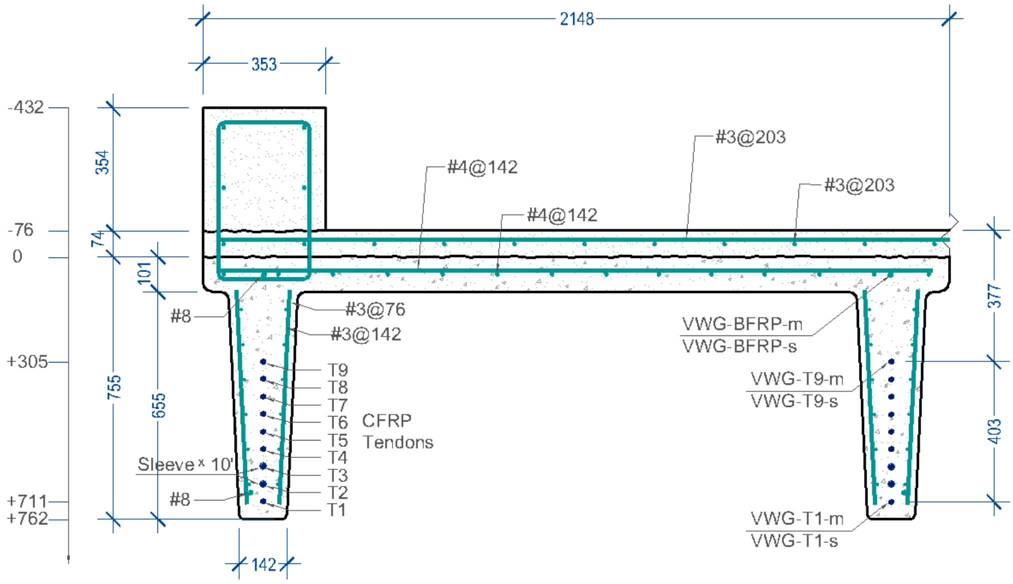

Figure 1. Cross section of the double tee with concrete topping and curb (measures in mm).

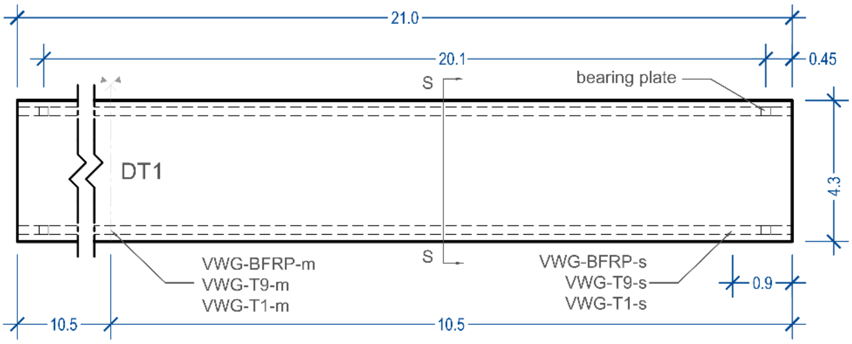

Figure 2. Plan view of the Double Tee 1 (measures in m).

3.2 Material stresses and DTs capacity

The imposed pre-stressing force intentionally exceed the threshold suggested by ACI 440.4R (2011). A stress corresponding to 68% of the CFRP guaranteed strength is applied on each strand at jacking, with the purpose of better exploiting the potential of CFRP tendons. The nominal flexural capacity of the girders is calculated considering the specified values of material properties and the full section of the girders after the concrete topping casting. As specified by ACI 440.1R, an environmental reduction factor (C_E) of 0.9 is adopted for CFRP composites in order to take into account for long-term exposure to the environmental loads. A step-by-step analytical procedure based on the model proposed by Naaman (2012) is adopted to compute concrete creep and shrinkage. A logarithmic relation based on experimental observations (Tokyo Rope Mfg Co Ltd 2014) was employed to calculate the CFRP relaxation. The resulting nominal flexural capacity and cracking moment of the single DT, including the concrete topping and curb, at the 75-year service life, are 3127 kN·m and 1424 kN·m, respectively. The factored flexural capacity of each girder, completed with concrete topping and curb, is 2575 kN·m, a value exceeding the demand of the structure at ultimate.

4 CONSTRUCTION

The DT precast girders were constructed and instrumented adopting a casting bed and pre-stressing equipment available for conventional steel strands. The tendons and the pre-fabricated meshes were handled without aid of mechanical equipment. All the reinforcement was installed and secured before the tensioning took places. As the PC elements were arranged in series, the tensioning was applied concurrently to the two girders.

4.1 Instrumentation

With the aim of monitoring the strains during the entire service life of the bridge, and measuring the effective strains and transfer lengths during construction, DT1 was instrumented with 6 Vibrating Wire Gauges (VWGs): 4 installed on the CFRP tendons and 2 installed on the BFRP reinforcement. As shown in Figure 1 and Figure 2, the top (T9) and the bottom (T1) tendons of a selected stem of DT1 were taken in consideration: 2 gauges were installed at the DT mid-span (VWG-T9-m and VWG-T9-s), whereas two more were installed at about 0.91 m from one of the end sections (VWG-T9-s and VWG-T9-s). Similarly, VWG-BFRP-m and VWG3-BFRP-s were installed on the BFRP longitudinal reinforcement in correspondence of the monitored stem, at DT mid-span and at 0.91 m from the same end section, respectively.

4.2 Tensioning

CFRP is a brittle material, sensitive to shocks caused by hard and sharp objects. Consequently, applying a tension force to CFRP using a mechanical device is a process that requires particular care. A conventional tensioning apparatus was used to pull steel cables connected to the CFRP strands through a proprietary mechanical anchorage system, which facilitated the splicing without causing localized damages. The device, shown in Figure 3, consists of two anchoring systems based on sleeves and wedges (one for CFRP and one for steel), connected by a coupler. Each CFRP tendon was equipped with a mesh sheet and a braided grip to protect it from damages. The tensioning force of 183.5 kN was monitored by means of a calibrated pressure transducer and verified by measuring the cables elongation as well as detecting the strains in the instrumented tendons. After the tensioning was completed, the SCC was poured.

4.3 Releasing

Steel strands are normally flame cut using a torch, in order to take advantage of the gradual energy release caused by the elevated temperature, which lowers the yielding point of steel. This kind of process cannot be adopted for FRP tendons that need to be severed by grinding.

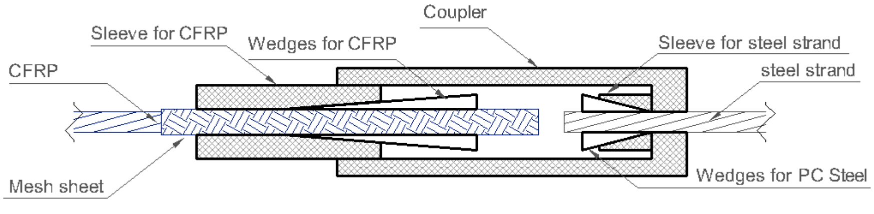

Figure 3. CFCC / PC strands anchorage system.

The tension was released at the two extreme sides of the tensioning bed by acting firstly on the steel rather than on CFRP strands. Following the end release, the CFRP strands in between the two DTs were carefully cut using a grinder. The release of the pre-stressing forces took place 24 hours after casting. At that time, the measured concrete compressive strength was 36.6 MPa. Following these operations, the girders were successively demolded.

5 LOAD TEST

In order to analyze the flexural response under service conditions, a static load test was carried out on the instrumented girder (DT1) at the precast yard, before its on-site installation. The test, conducted according to a three-point loading scheme, over the 20.1 m effective span took place 26 days after casting.

5.1 Test Arrangement

The test load magnitude was designed in order to avoid concrete cracking. The analytical procedure was refined accounting for the actual properties of the concrete employed and the progressive gain of strength/stiffness due to aging (Table 1). This resulted in a 120 kN test load in addition to the self-weight. The test condition corresponds to the 85% of the DT cracking moment, computed per ACI 318 (2014) recommendations and accounting for concrete gain in strength over time.

Table 1. Deflection at mid-span and girder camber (absolute values)

	Experimental values mm	Analytical prediction mm	Error %
Elastic deflection (120 kN – 0 h)	27.33	27.76	+2%
Additional deflection (120 kN – 24 h)	2.95	2.64	+12%
Residual Deflection (120 kN – 24 h)	3.43	2.64	+30%
Initial camber (26 days)	49.71	46.81	-6%
Post-test camber (27 days)	46.30	44.15	-5%

As shown in Figure 4, three rectangular concrete blocks, each of them weighting 40 kN, were used to apply the intended load by means of a crane. The DT girder displacements were monitored using 10 analogic Dial Gauges (DG), installed in correspondence of the two stems. Dial gauges 1, 2, 3 and 4 were used to monitor the supports settlement; Dial gauges 7 and 8 were aimed to measure the DT deflection at mid-span whereas Dial Gauges 5, 6, 9, and 10, were positioned symmetrically at the quarter spans.

Figure 4. DT girder loaded under a three-point-load setup.

The 120.10 kN total load was applied in three steps. After applying one block, the second and third concrete blocks were positioned on the DT girder, successively removed and then permanently repositioned on the girder mid-span. The total load was sustained over a 24-hour period. The loading and unloading phases required about 2 hours each. The dial gauges measurements were monitored at each load step.

6 RESULTS AND DISCUSSION

Figure 5 shows the experimental load vs. mid-span/quarter-span deflection diagrams obtained during the 24-hour loading cycle. The analytical prediction of the load vs. mid-span deflection curve is also depicted on the diagram.

The girder exhibited the elastic performance expected under loading corresponding to service conditions, with no visible cracking. Due to the sustained 120 kN load, additional deformations mainly resulting from concrete creep) were observed during the 24-hour monitoring. As can be observed in Table 1, the observed elastic deflection at 120 kN and additional deflection after 24 h of sustained load are consistent with analytical prediction (errors of +2% and +12%, respectively). The experimental value of the residual deflection immediately after the load removal is instead considerably higher than predicted (error of +30%), probably because elastic recovery is not instantaneous. Similar considerations apply to the measurement performed on the girder camber. The predicted analytical values of the camber only deviate +6% and +5% from the values measured before and after the performance of the load test, respectively, with the experimental absolute values being slightly higher than the ones expected.

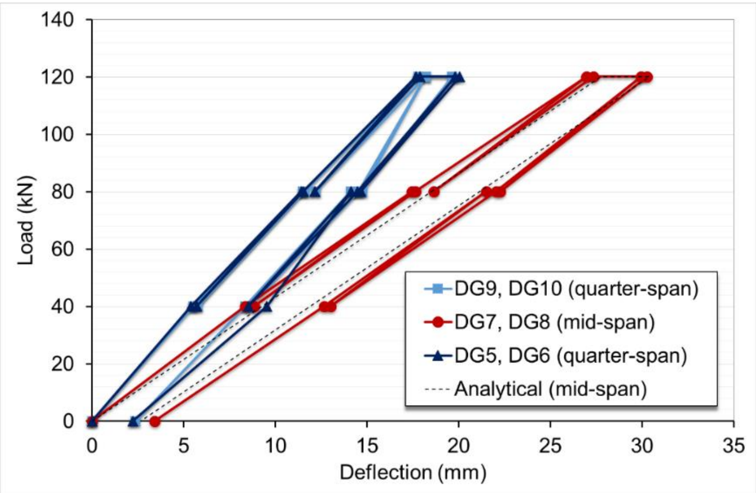

Figure 5: Load-Deflection diagrams.

The deflection profiles of the girder at the different loading phases and the corresponding analytical curves are plotted in Figure 6. Also in this case, the theoretical modeling appears fully capable to describe the behavior of the structural element at the monitored sections and for different levels of loads.

Figure 7 illustrates the measured strain profile at the girder mid-span section and the analytical prediction of elastic strains corresponding to the 120 kN loading. The experimental data detected on tendons are in satisfactory agreement with the theoretical values and show the expected linearity of the strains along the mid-span cross section. The strains measured on bottom (T1) and the top (T9) tendons differ by +3% and -6%, respectively from the analytical predictions. Only the strain measured on the BFRP mesh is considerably higher than the predicted analytical value (+36%).

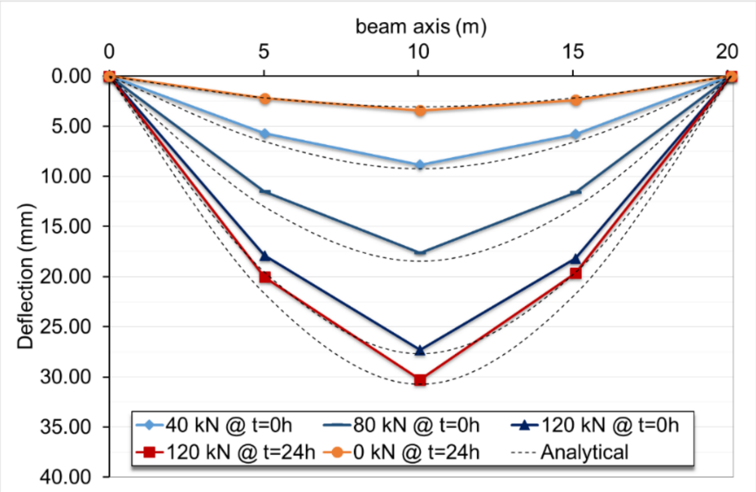

Figure 6: Deflection profile along the beam axis.

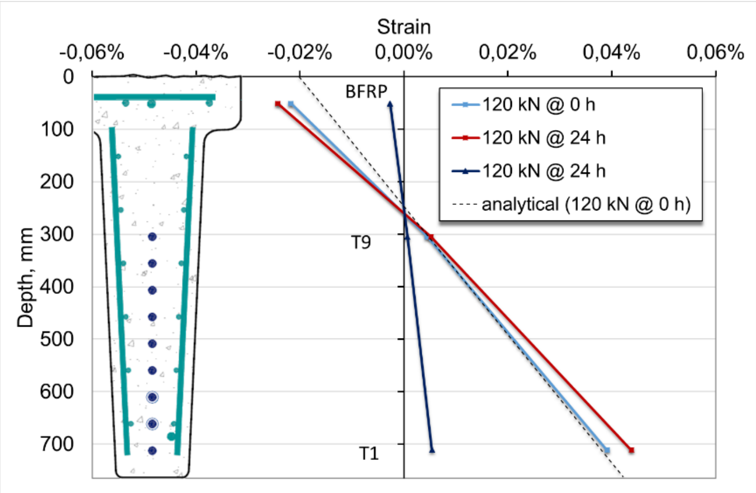

Figure 7: Measured strain profile at DT1 mid-span.

Figure 8 shows one of the DT girders during lifting and loading phases.

Figure 8: DT girder being loaded into place.

7 CONCLUSIONS

Assumptions traditionally used for steel-PC were adopted for the design of thin walled CFRP-PC sections, leading to construction details very similar to those requested to analogue steel-PC structures in order to resist the same loads. In spite of this, some differences have arisen with respect to the tensioning procedure.

A mechanical anchoring system able to facilitate pulling of the strands without damaging them allowed us to attach the CFRP tendons to PC steel cables and consequently use a conventional tensioning apparatus. In this view, the great flexibility of the method was recognized in consideration of the limited deployment of FRPs strands in the construction market, and the consequent unavailability of tensioning equipment in precast plant. CFRP tendons showed a mechanical efficiency comparable to standard steel strands, thanks to a higher guaranteed load, elastic behavior up to failure and a lower elastic modulus, resulting in reduced losses. Increasing the level of pretension over the current ACI 440.4R limit and using 15.2 mm diameter CFRP tendons in the thin stems of double tees are the key factors to effectively exploit the properties of such materials. All calculations have been performed with reference to established theories and mechanical models, proving that the implementation of CFRP tendons would not require any additional design efforts from practitioners. The response of the DT to the static load test have demonstrated the reliability of the analytical predictions. Strains and deformations observed over time appear to be largely dominated by the rheological behavior of concrete. As expected, CFRP tendons relaxation phenomena do not seem to visibly affect the deformation of the girders.

The study overall demonstrates that CFRP pre-stressing technology can be successfully employed on thin walled concrete sections without evident technological drawbacks compared to the use of steel reinforcement and over the threshold imposed by current guidelines. Future work will focus on the long-term monitoring of the Innovation Bridge. A standard procedure has been defined for strain and camber monitoring over the bridge 75-year service life, load tests are also scheduled to periodically verify the structures behavior in service condition.

REFERENCES

AASHTO LRFD (2009). "Bridge design guide specifications for GFRP-reinforced concrete bridge decks and traffic railings." American Association of State Highway and Transportation Officials, Washington, DC.

ACI 318 (2014). *Building Code Requirements for Structural Concrete and Commentary (Metric)*, American Concrete Institute.

ACI 440.1R (2015). "Guide for the Design and Construction of Structural Concrete Reinforced with Fiber-Reinforced Polymer (FRP) Bars." American Concrete Institute, Farmington Hills, MI.

ACI 440.3R (2012). "Guide Test Methods for Fiber-Reinforced Polymers (FRPs) for Reinforcing or Strengthening Concrete Structures." American Concrete Institute, Farmington Hills, MI.

ACI 440.4R (2011). "Prestressing Concrete Structures with FRP Tendons (Reapproved 2011)." American Concrete Institute, Farmington Hills, MI.

Burke, C. R., and Dolan, C. W. (2001). "Flexural design of prestressed concrete beams using FRP tendons." *PCI Journal*, 46(2), 76-87.

Grace, N. F. (2000). "Transfer length of CFRP/CFCC strands for double-T girders." *PCI Journal*, 45(5), 110-126.

Naaman, A. E. (2012). *Prestressed Concrete Analysis and Design: Fundamentals.*, Techno Press 3000.

Nanni, A., Claure, G., De Caso y Basalo, F. J., and Gooranorimi, O. (2016). "Concrete and Composites Pedestrian Bridge." *Concrete International*, 38(11).

Spadea, S., Orr, J., Yang, Y., and Nanni, A. (2017). "Wound FRP shear reinforcement for concrete structures." *Journal of Composites for Construction*.

Tokyo Rope Mfg Co Ltd (2014). "Report for Long Term Relaxation of CFCC 1x7 15.2ϕ."

Ushijima, K., Enomoto, T., Kose, N., and Yamamoto, Y. (2016). "Field deployment of carbon-fiber-reinforced polymer in bridge applications." *PCI Journal*, 61(5), 29-36.